THE JOURNAL OF BIOLOGICAL CHEMISTRY VOL. 285, NO. 48, pp. 37531–37541, November 26, 2010

CD23 Sheddase A Disintegrin and Metalloproteinase 10 (ADAM10) Is Also Required for CD23 Sorting into B Cell-derived Exosomes*[S]

Received for publication, May 24, 2010, and in revised form, September 7, 2010 Published, JBC Papers in Press, September 28, 2010, DOI 10.1074/jbc.M110.141556

Joel A. Mathews[‡], David R. Gibb[‡], Bing-Hung Chen[§], Peggy Scherle[¶], and Daniel H. Conrad[‡1]

From the [‡]Department of Microbiology and Immunology, Virginia Commonwealth University School of Medicine, Richmond, Virginia 23298, the [§]Department of Biotechnology, Kaohsiung Medical University, Kaohsiung 807, Taiwan, and [¶]Incyte Corporation, Wilmington, Delaware 19880

The low affinity receptor for IgE, CD23, is the natural regulator of IgE synthesis, and understanding both the synthesis and the catabolism of CD23 are, thus, important issues. Membrane CD23 is cleaved by a disintegrin and metalloproteinase 10 (ADAM10) and this cleavage influences the ability of CD23 to regulate IgE. In contrast to the belief that cleavage is a cell surface event, endosomal neutralization with NH_4Cl was found to dramatically reduce CD23 cleavage, suggesting that the majority of CD23 cleavage occurred subsequent to internalization in the endosomal pathway and not at the cell surface. In line with this, full-length CD23 was shown to be sorted in an ADAM10-dependent manner into exosomes. Greatly increased ADAM10-mediated CD23 cleavage was seen at endosomal pH. Additionally, the stalk region of CD23 was found to interact with ADAM10 and ADAM10 binding of CD23 was found to be protease independent. SPR analysis of the interaction indicated about a 10-fold increase in the R_{max} at endosomal pH (pH 5.8) compared with pH 7.4, whereas the affinity of the interaction was not significantly changed. The R_{max} change, combined with the increased cleavage at endosomal pH, indicates greater accessibility of the CD23 stalk region for ADAM10 at the lower pH. These results indicate a model where CD23 internalization results in ADAM10-dependent incorporation into exosomes, followed by partial cleavage of CD23 by ADAM10 prior to being released from the cell. The increased cleavage at endosomal pH also has implications for other ADAM10 substrates.

The cleavage of plasma membrane-bound proteins and their subsequent release from the cell is described as ectodomain shedding. Historically this was believed to be a cell surface process. However, recently a second mechanism was discovered, involving the release of proteins after their internalization and subsequent trafficking through the endosomal pathway to multivesicular bodies (MVB)[2] (1). In the MVB, the proteins can interact with their sheddase and be cleaved and released or be sorted into exosomes and released as full-length proteins. Exosomes are small, 30–100 nm, membrane containing vesicles that are released by a wide variety of cells. As they have high expression of major histocompatibility complexes (MHC) molecules they have been investigated as cell-free transporters of cancer antigens in cancer immunotherapy treatments (2). Exosome released from B cells have also been extensively studied. B cell-derived exosomes express integrins (3), which allow them to bind, and potentially present antigen to T cells. They also transport antigens, including peptides derived from allergen between antigen presenting cells (reviewed in Ref. 4). B cell exosome secretion is also increased upon activation (5) and interaction with T cells (6). However, the secretion of exosomes by cells as well as the mechanism that controls the sorting of proteins into exosomes are still poorly understood.

The low-affinity receptor of immunoglobulin E (CD23) is an important regulator of IgE production and the allergic response. CD23 (48 kDa for mice, 45 kDa for human), a type II integral membrane protein, is composed of a C-terminal lectin head, a leucine zipper, a transmembrane domain, and a short cytoplasmic tail. In addition to being a membrane-bound protein, CD23 can also be cleaved and is found in sera of allergic patients and B cell cultures (reviewed in Ref. 7). Because CD23 cleavage enhances IgE production (8) and given the IgE regulation seen with the intact molecule, blocking cleavage of CD23 represents a potential way to inhibit IgE synthesis and ultimately, type I allergic disease. Soluble CD23 (sCD23) retains IgE-binding ability, although at much lower affinity/avidity than membrane trimeric CD23. In humans, the sCD23 interaction with CD21 on B cells has been reported to cause increased IgE production (9). Through its interaction with macrophage-bound CD11/CD18, it causes the release of pro-inflammatory cytokines, *i.e.* IL-1 and TNF (10). Membrane-bound CD23 through the use of knock-out and transgenic animals has been shown to regulate IgE synthesis. Thus, anything that promotes membrane CD23 as well as decreases sCD23 would be expected to enhance the CD23 regulatory activity of IgE as well as decrease inflammation induced by sCD23. IgE (11) and monoclonal anti-CD23 that are directed against the lectin domain

* This work was supported, in whole or in part, by National Institutes of Health Grants RO1AI18697 and 1U19AI077435 and imaging cytometry supported by Grant P30 CA16059.

[S] The on-line version of this article (available at http://www.jbc.org) contains supplemental Figs. S1–S3.

[1] To whom correspondence should be addressed: P.O. Box 980678, Virginia Commonwealth University, Richmond, VA 23298. Fax: 804-828-9946; E-mail: dconrad@vcu.edu.

[2] The abbreviations used are: MVB, multivesicular bodies; ADAM10, a disintegrin and metalloproteinase 10; sCD23, soluble CD23; HBS, Hepes-buffered saline; TBS, Tris-buffered saline; SPR, surface plasmon resonance; *Iz*-CD23, leucine zipper-trimerized recombinant CD23; MES, 4-morpholineethanesulfonic acid.

(12) both protect CD23 from cleavage and thus, decrease IgE production; these reagents are termed CD23 stabilizing antibodies. Monoclonal antibodies that are directed against the stalk region of CD23 have been shown in both human (12) and mouse (8) to enhance CD23 cleavage, as well as enhance IgE production. As such, they are called CD23 destabilizing antibodies. These results led to the hypothesis that the stability of CD23 modulates its IgE regulatory activity. This hypothesis assumes that CD23 cleavage is occurring primarily at the cell surface.

In 2006, our laboratory reported that the protease primarily responsible for the cleavage of CD23 was ADAM10 (13); this cleavage forms fragments of 35 and 37 kDa in mice and humans, respectively. After this first cleavage, sCD23 undergoes additional proteolysis, to form fragments of 33, 25, and 16 kDa. The initial ADAM10-dependent cleavage was believed to take place at the cell surface; however, high levels of ADAM10 are seen in the Golgi and the endosomal regions of the cell. Indeed two of the substrates of ADAM10, CD44 and the adhesion molecule L1 (CD171), were recently shown to be cleaved and released in exosomes (14), which indicates an alternative mechanism for ADAM10 substrate trafficking and cleavage.

In this study, ADAM10 cleavage of CD23 was further characterized; including the examination of the hypotheses that CD23 is cleaved at the surface and that the stability of CD23 affects the ability of ADAM10 to bind. We found that ADAM10-mediated cleavage was greatly enhanced by CD23 internalization into endosomes and that intact CD23 is incorporated, in an ADAM10-dependent manner, into exosomes. Cleavage, once incorporated into exosomes, is very rapid at endosomal pH. Thus, CD23 is analogous to the previously mentioned ADAM10 substrates, L1 and CD44, in terms of its primary site of ADAM10 interaction and substrate cleavage. The data also indicate that stabilizing mAbs work by retaining CD23 at the cell surface and destabilizing mAbs work by increasing CD23 internalization. The implications for these findings in terms of IgE regulation are also discussed.

EXPERIMENTAL PROCEDURES

Reagents—FITC rat anti-mouse CD23 (clone B3B4), an anti-lectin mAb, was obtained from BD Pharmingen. Rat anti-mouse CD23 (clone 2H10) (15), an anti-CD23 lectin mAb, 19G5 (15), an anti-CD23 stalk mAb and C0H2, a rat IgG2, used as an isotype control mAb, were all purified from tissue culture supernatant as previously described (16). Monoclonal mouse IgE (mIgE-DNP) (17) from H1-DNP-ϵ-26 was purified from tissue culture supernatant as described previously (16). Rabbit anti-ADAM10 was obtained from Chemicon (Billerica, MA). Rabbit anti-human CD23 was created in our laboratory by injecting recombinant trimeric human CD23 (*lz*-CD23) (15) containing the extracellular region of human CD23 into rabbits. The antibodies were then purified on a Protein G-Sepharose (Sigma) column. Mouse *lz*-CD23 (extracellular CD23 held in a trimer by the addition of a leucine zipper motif) and fragments, and yellow fluorescent protein (YFP) tagged mouse CD23 were created as previously described (18). The ADAM10 inhibitor, INC8765 (19), was synthesized by Incyte Corporation (Wilmington, DE). HA-ADAM10-pcDNA3.1 (20) was a gift from Carl Blobel at Cornell University. Dominant-negative ADAM10 lacks its metalloproteinase domain and consists of the leader sequence and part of the prodomain linked to the disintegrin, cysteine-rich, transmembrane and cytoplasmic domains were produced as described (21) and inserted into p-Tracer. Rabbit anti-HA was purchased from Novus Biologicals (Littleton, CO). Goat anti-rabbit HRP was obtained from Southern Biotech (Birmingham, AL). A humanized anti-lectin human CD23 (IDEC-152) (22) was a gift from Marylin Kehry at Biogen-Idec (San Diego, CA). Ez-link-sulfo-NHS-biotin (NHS-biotin) was purchased from Pierce. Anti-H2-I/Adβ (5K43) was purchased from Santa Cruz Biotech (Santa Cruz, CA). Mouse IL-4 was a gift from Bill Paul (National Institutes of Health). Rabbit anti-calnexin (BD Biosciences), goat anti-EEA1 (Santa Cruz), rabbit anti-Rab11 (Invitrogen), and mouse anti-LAMP1 (University of Iowa hybridoma bank) were all gifts from Dr. Jason Carylon (Virginia Commonwealth University). DyLight 649-donkey anti-rabbit IgG and DyLight 649-goat anti-mouse IgG were purchased from BioLegend (San Diego) and allophycocyanin rabbit anti-goat IgG from BD Biosciences. PE-goat anti-rabbit IgG and FITC-goat anti-rat IgG were also purchased from BioLegend. Recombinant mouse ADAM10 (rADAM10) was purchased from R&D Bioscience (Minneapolis, MN).

Mice—CD19-Cre$^{+/-}$ADAM10$^{fl/fl}$ mice on a C57BL/6 background (24) were described previously, and were used as a source of ADAM10-deficient B-cells, littermates that were negative for Cre expression were used as WT controls. All mouse protocols were approved by the Virginia Commonwealth University Institutional Animal Care and Use committee.

Cell Culture—293T cells were a gift from Dan McVicar (National Cancer Institute, Frederick, MD), and grown in complete DMEM (10% FBS (Gemini Bio-Products, West Sacramento, CA), 100 units/ml of penicillin and streptomycin, and 2 mM L-glutamine (all from HyClone, Logan, UT). They were transiently transfected using FuGENE 6 with mouse CD23-YFP (15) to study the effects of CD23 stability on internalization and localization. The 293 variant (293-F) was purchased from Invitrogen and grown and transiently transfected with mouse ADAM10-HA contained in pCDNA3.1 according to the manufacturer's protocol. Mouse CD23$^+$-CHO (mCD23$^+$-CHO) cells were made as previously described and grown in DMEM-GS (25) and were used to examine internalization of mouse CD23 as well as exosome formation. RPMI 8866 cells were maintained as described (13). Mouse B-cells were isolated by sorting with anti-B220 and stimulated with 10 μg/ml of LPS (Sigma) and 25 ng/ml of IL-4. CD23$^+$-ADAM10 null mouse embryonic fibroblasts were a gift from Carl Blobel (13).

Fluorescence Imaging—mCD23$^+$-CHO cells were plated at a concentration of 2×10^5 cells/ml on glass coverslips previously coated with 0.1 mg/ml of polylysine (sigma) and allowed to bind. FITC-B3B4 was then added at 4 °C and after 30 min internalization was initiated by transferring the cells to 37 °C for the time indicated. Cells were then fixed with FCM fixation buffer (Santa Cruz biotechnology) and adhered to microscope slides using Prolong Gold Antifade Reagent (Invitrogen). Imaging was performed under oil immersion at ×100 on a Zeiss AxioObserver.Z1 with an integrated MRm Camera and analyzed with Axiovision 4.63 software (Carl Zeiss,

Inc., Thornwood, NY). 293T cells transiently transfected with mouse CD23-YFP were also plated on polylysine-coated coverslips. After 24 h the following antibodies were added 19G5 (destabilizing), 2H10 (anti-lectin, stabilizing), IgE, or IgG control and after an additional 24-h incubation, cells were then fixed and imaged and the percentage of cells with internalization was determined by looking at orthogonal views. In addition these same cells were stained with antibodies against specific intracellular compartments, with antibodies against the following antigens: EEA-1 for early endosomes (26), LAMP-1 (27) for lysosomes, Rab11 (28) for recycling endsomes/MVB, and calnexin for ER (29). The percentage of cells with co-localization was determined, with a cell being counted as positive if any co-localization in the cell was determined.

Mouse sCD23 Release Studies—mCD23$^+$-CHO were plated at 1×10^6/ml in 6-well plates and allowed to adhere. After incubation for 30 min with 10 mM NH_4Cl the cells were incubated with either 19G5 or IgE for 8 h. sCD23 in the supernatants was determined by ELISA (15) with 2H10 (rat anti-mouse CD23 antibody) as the coating antibody and rabbit anti-mouse CD23 for detections. EC-mCD23 (recombinant extracellular mouse CD23) was prepared in our laboratory and used as a standard.

Dot and Western Blots—For dot blots, *lz*-mCD23 starting at 20 μg/200 μl of PBS was serially diluted 1:2 across a Hybrid-Dot Manifold (Invitrogen) containing nitrocellulose (Pall Corp., Pensacola, FL) and excess liquid was removed by applying vacuum. The nitrocellulose containing CD23 was then removed from the apparatus and blocked in 5% milk in 1× HBS and 0.05% Tween 20. Blots were then incubated with 19G5, IgE, or nothing. Following washing, cell lysate from 293F cells that had been transiently transfected with HA-ADAM10 (transfection was confirmed by Flow Cytometry and Western blot (data not shown)) expression vector 2 days previously were added and blots were incubated overnight at 4 °C. ADAM10 binding was then detected using a rabbit anti-ADAM10 and a goat anti-rabbit HRP.

For mouse and human CD23 dot and Western blots, CD23 was detected with either rabbit anti-human or rabbit anti-mouse CD23 followed by goat anti-rabbit HRP. For ADAM10 and MHC class II blots, the respective proteins were detected using rabbit anti-ADAM10 and anti-H2-I/Adβ followed by their respective HRP-conjugated secondary antibodies.

Immunoprecipitation and Biotinylation—Human CD23 contained in the supernatant or exosomes was precipitated with either IDEC-152 in combination with Protein A/G or avidin-agarose and analyzed by Western blot. For biotinylation experiments, RPMI 8866 cell surface proteins were biotinylated as described by the manufacturer (Pierce). Briefly cells were suspended in 1× HBS containing 50 μg/ml of NHS-biotin for 30 min at 4 °C and then washed three times in 1× Tris-buffered saline (TBS) to remove unbound biotin. Cells were then grown for 24 h and exosomes were isolated as described below. Exosomes were lysed for 10 min on ice in 1× HBS containing 0.5% Nonidet P-40 and a complete protease inhibitor mixture tablet (Roche). Biotinylated proteins were then isolated with avidin-agarose and analyzed for CD23 by Western blot. For mouse CD23 precipitation, 2H10-Affi-Gel (Bio-Rad) was used, 2H10 was coupled to Affi-Gel according to the manufacturer's instructions.

Isolation of Exosomes—Exosomes were isolated as previously described (14). The cell sources were RPMI 8866 or mCD23$^+$-CHO cultured overnight or primary mouse B cells cultured for 3 days with IL-4 and LPS. Briefly cells were pelleted by spinning them at $350 \times g$ for 5 min and supernatants were harvested. To remove any possible apoptotic bodies the supernatants were spun at $27{,}000 \times g$ for 20 min. Finally exosomes were harvested by spinning at 1×10^5 x g for 1 h; the exosome pellet was resuspended in 5 ml of PBS and pelleted again using ultracentrifugation (Sorvall AH-650 rotor). Some samples were then suspended in HBS and layered over a discontinuous sucrose gradient using concentrations of 2, 1.3, 1.16, 0.8, 0.5, and 0.25 M sucrose in HBS at $1 \times 10^5 \times g$ for 17 h. After centrifugation 1-ml fractions were removed starting at the top and diluted in 4 ml of HBS. Fractions were then spun at $1 \times 10^5 \times g$ for 1 h using the Sorvall AH-650 rotor to pellet vesicles. Pelleted exosomes were then suspended in an equal volume of PBS with SDS and reducing agent and boiled; the presence of CD23 and ADAM10 were then detected via Western blot as described above.

Surface Plasmon Resonance (SPR)—The association of mouse CD23 with rADAM10 was measured by SPR using a Biacore T100 optical biosensor (GE Healthcare). Lane one of a CM5 sensor chip (series S CM5; GE Healthcare) was activated, then blocked with ethanolamine; in the second lane, rADAM10 (10 μg/ml diluted in 0.01 M acetate, pH 4.5) was immobilized to an equivalent of 1500 resonance units and then blocked with ethanolamine. Recombinant *lz*-CD23 (amino acids, 139–331 (18)) at a flow rate of 30 μl/min was passed over the chip at concentrations of 5–100 μg/ml diluted in either 10 mM Hepes-buffered saline, pH 7.4, containing 2 mM CaCl and 0.05% (v/v) surfactant-P20 or 50 mM MES-buffered saline, pH 5.8, containing 2 mM CaCl and 0.05% (v/v) surfactant P-20, and binding was recorded. The response from the control lane was subtracted and affinity and R_{max} was determined using Biacore evaluation software version 1.1 using steady state analysis. To determine the amount of recombinant CD23 that renatured correctly, binding to IgE Affi-Gel was determined as described previously (30). The purified recombinant *lz*-CD23 protein concentration was adjusted by this percentage.

Statistical Analysis—All statistics were done using the Student's two-tailed *t* test. In the case of Fig. 1*c* Bonferroni correction was also used. All error bars represent standard deviation.

RESULTS

Correlation between CD23 Internalization and CD23 Cleavage—CD23 binding reagents have been defined previously according to whether they decreased or increased CD23 cleavage, these two activities were called stabilizing or destabilizing, respectively (15). To further investigate this phenomena, we first sought to confirm studies (31, 32) that showed that anti-CD23 cause ligand internalization. mCD23$^+$-CHO cells were labeled with FITC-anti-CD23 (FITC-B3B4), which is an anti-lectin mAb, transferred to 37 °C and internalization was followed (Fig. 1*B*). Examination of orthogonal views demonstrated that the visualized punctate spots were found inside the cell after 30 min, whereas at 4 °C (Fig. 1*A*) they were still at the

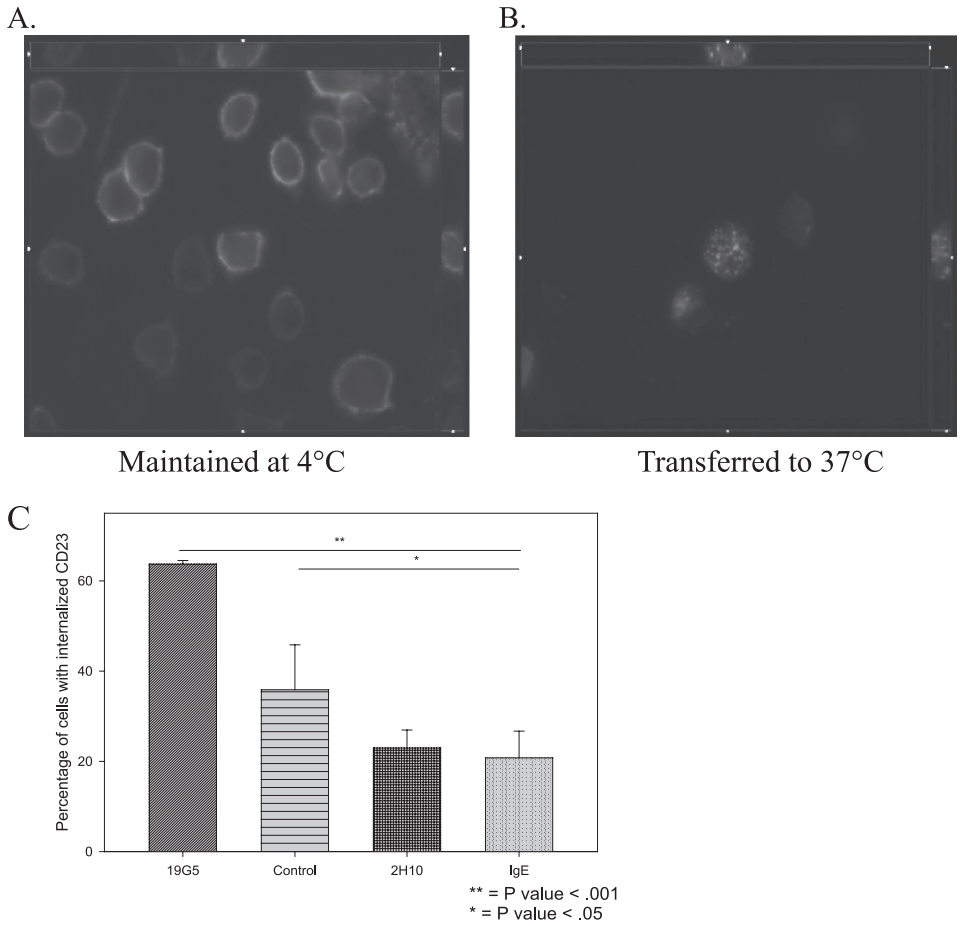

FIGURE 1. **Effect of anti-CD23 stalk *versus* anti-lectin and IgE on CD23 internalization.** mCD23$^+$-CHO (25) were plated on polylysine-coated coverslips and allowed to adhere. After staining with a FITC rat anti-mouse CD23 lectin (B3B4) for 30 min at 4 °C, cells were either (*B*) transferred to 37 °C for 30 min or (*A*) left at 4 °C. *C*, to test if the stability of CD23 affected the amount of internalization. HEK293T cells transfected with mouse CD23-YFP were plated on coverslips and surface CD23 was either stabilized by the addition of either 2H10 (anti-lectin) or IgE, destabilized with 19G5, or left untreated as a control. The percentage of cells where CD23 was internalized was calculated after a 24-h incubation (37 °C). Bonferroni adjustment was used to check for significance. *A* and *B* data are representative micrographs from three experiments of similar design and *C* data are averaged from four independent experiments.

TABLE 1

Internalized CD23 localizes to endosome compartments

HEK293T cells were transiently transfected with CD23-YFP and examined for CD23 internalization after 48 h. Cells were then stained with antibodies against different cellular compartments and their respective secondary antibodies. Percentage of cells with co-localization was determined, with a cell being counted as positive if any co-localization was determined. Data are the average of three independent experiments.

Marker	Compartment	Co-localization with CD23
		%
Calnexin	ER[a]	11.7 ± 0.71
Early endosomal Ag	Endosome	72.1 ± 18.5
LAMP1[b]	Lysosome	21.2 ± 8.8
Rab11	Recycling endosomes/MVB	95.1 ± 4.4

[a] ER, endoplasmic reticulum.
[b] LAMP1, lysosome-associated membrane protein 1.

cell surface; thus, showing that CD23 is internalized following anti-lectin binding. To determine whether there was a correlation between CD23 cleavage and internalization, 293T cells were transfected with CD23-YFP. Previous studies had shown that stabilizing CD23 with IgE or anti-lectin antibodies decreased CD23 cleavage, whereas destabilizing antibodies increased cleavage (8, 12). The CD23-YFP expressing 293T cells were then incubated with the indicated antibodies for 24 h and examined by immunofluorescence. The percentage of cells with internalized CD23 was then determined and the data are summarized in Fig. 1*C*. We found that significant CD23 internalization occurs naturally even in the absence of ligand, however, anti-stalk mAbs (19G5) increased this internalization, whereas IgE and the anti-lectin (2H10) decreased internalization compared with this control. Of note with anti-lectin mAbs and IgE, there still is internalization (Fig. 1*C*) but it was decreased compared to control. As the anti-lectin and IgE were also found to act similarly, only IgE was used throughout the rest of the study. These data suggests that the stability affect on cleavage could be related to internalization. In additional studies, co-staining with antibodies against markers of different subcellular compartments was performed. This data are summarized in Table 1. CD23 co-localization with EEA1 and Rab11 indicates endosomal trafficking and is in agreement with previous work that showed that CD23 traffics through the endosomal pathway (31, 32).

Enhanced Internalization Correlates with Enhanced sCD23 Production—Previous studies have shown that subsequent to the internalization of CD23-bound IgE-antigen complexes, some CD23 eventually recycled back to the cell surface (31). Thus, to determine whether internalized CD23 as seen in Fig. 1 was related to the fragments found in the supernatant or is recycled, cells were treated with antibodies that stabilize (IgE) or destabilize (19G5) CD23 ± NH_4Cl. NH_4Cl prevents the progression of proteins in the endosomal pathway by neutralizing the endosomal pH (33). As shown in Fig. 2*A*, the enhanced CD23 cleavage that is characteristic of the anti-stalk mAb, 19G5 (8), is reversed in the presence of 10 mM NH_4Cl. In contrast, NH_4Cl treatment of mCD23$^+$-CHO where CD23 was stabilized with monomeric IgE had no affect with respect to sCD23 production (Fig. 2*B*). Note also that the amount of sCD23 released into the supernatant was significantly lower in cells where CD23 was stabilized compared with cells where CD23 had been destabilized. NH_4Cl treatment brought sCD23 release from cells in which CD23 was destabilized down to levels only 1.5 times (30 *versus* 18 ng/ml) higher than that released from cells where CD23 was stabilized. In addition, this inhibition of enhanced CD23 cleavage is similar to what was seen with an ADAM10 inhibitor (13). A similar trend was also seen with primary human B cells in which both

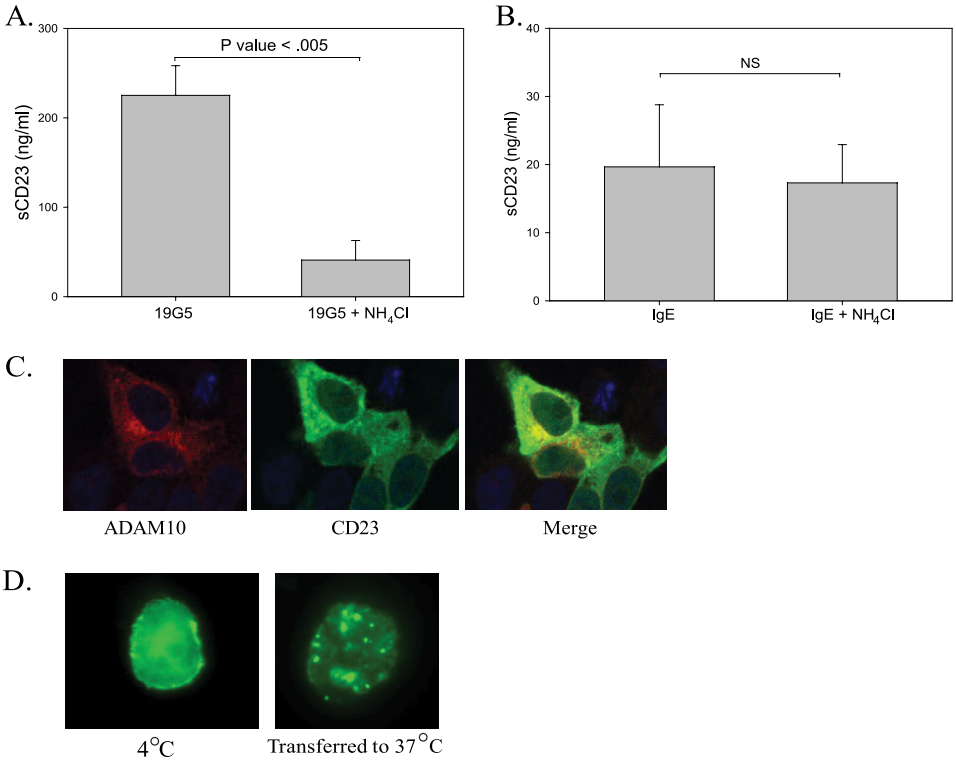

FIGURE 2. **Intracellular compartments are important for the release of CD23 fragments.** sCD23 ELISA of an 8-h culture supernatant of mCD23$^+$-CHO cells ± 10 mM NH_4Cl treatment; shown is the average of two independent experiments. CD23 cleavage was induced by the addition of a destabilizing antibody, 19G5 (*A*) or inhibited by the addition of IgE (*B*). *C*, ADAM10-HA and CD23 doubly transfected HEK293T cells were grown on coverslips and incubated with rabbit anti-HA (*red*) and rat anti-mouse CD23 (*green*); after washing detection was with PE-anti-rabbit IgG and FITC anti-rat IgG. *D*, CD23 stably transfected mouse embryonic fibroblasts derived from ADAM10$^{-/-}$ embryos (13) were stained with FITC-B3B4 and either left at 4 °C or transferred to 37 °C and examined after 30 min. Each panel is representative of at least two independent experiments.

NH_4Cl (data not shown) and inhibition of ADAM10 (13) caused a 50% drop in sCD23. Thus, when internalization was inhibited, as seen with IgE in Fig. 2*B*, the NH_4Cl effect is minimal and the converse is true when internalization is enhanced. To ensure that NH_4Cl was not simply blocking internalization, mCD23$^+$-CHO cells were stained with FITC-anti-CD23 in the presence or absence of NH_4Cl and then internalization was allowed to continue (supplemental Fig. S1). This shows that NH_4Cl does not block ligand-induced internalization and that the affect of NH_4Cl is related to neutralization of the intracellular compartments.

As stated in the Introduction, the primary site of CD23 cleavage was thought to be the cell surface. Conversely, our data indicates that a majority of CD23 is internalized before it is released from the cell (Fig. 1*C*). To determine where CD23/ADAM10 co-localization occurred, 293T cells were doubly transfected with ADAM10-HA and CD23. After 24 h the cells were co-stained for CD23 and ADAM10 (Fig. 2*C*). CD23 was evident both on the cell surface and inside the cell. In contrast, ADAM10 was found mostly intracellularly, consistent with other reports (34). Co-localization was also primarily intracellular. This internal co-localization was also demonstrated using RPMI 8866 cells, a human B-cell line (data not shown). This led us to hypothesize that ADAM10 has no role in the internalization of CD23. To confirm our hypothesis that CD23 internalization did not require ADAM10, CD23$^+$-ADAM10$^{-/-}$ mouse embryonic fibroblasts were cultured with FITC-B3B4 as described in Fig. 1, *A* and *B*, and clear internalization was seen when bound by anti-CD23 (Fig. 2*D*). Overall this figure shows that NH_4Cl blocks the ability of ADAM10 and CD23 to interact intracellularly, suggesting that low pH might affect their interaction.

Full-length CD23 Is Incorporated into Exosomes—Recent reports have shown that multiple surface-bound proteins, including MHC class I and II, and the B cell receptor can be internalized and released from cells in the form of exosomes (4). To determine whether CD23 was also incorporated and/or released in exosomes, standardized numbers of RPMI 8866 cells were pelleted and exosomes were isolated from the cell-free supernatants by ultracentrifugation as indicated under "Experimental Procedures." The pellet was resuspended and subjected to sucrose density gradient ultracentrifugation. Fractions were collected and examined by Western blot (Fig. 3*A*). CD23 was found localized to the 1.12–1.16 M sucrose region, which is known to be where exosomes are found (34). The 1.3–2 M sucrose region, where membrane blebs localize, did not contain CD23. As exosomes have been shown to express ADAM10 (35), as a positive control the same fractions were also stained with anti-ADAM10 and a 60-kDa protein, which corresponds to mature ADAM10, was detected (Fig. 3*B*). Thus, both ADAM10 and CD23 were clearly associated with exosomes. Note that CD23 is full-length in that the molecular mass is 45 kDa, the same as that precipitated directly from cell lysates (Fig. 3*C*). This would be expected, because membrane CD23 would be incorporated. Fig. 3*D* represents an experiment where full-length mouse CD23, from CD23$^+$-CHO cells, is also shown to be found in exosomes. For Fig. 3*D*, CD23 internalization was first stimulated by a 16-h culture with the anti-stalk antibody, 19G5. The higher molecular mass of the two bands seen corresponds to full-length CD23 (see Fig. 3*D*) and that band is also seen when examining cell surface CD23 isolated from surface-biotinylated cells (not shown). The identity of the lower molecular weight band corresponds to EndoH-insensitive CD23 (36), and is, thus, presumably newly synthesized CD23. Note also that CD23 inclusion in exosomes is not just an artifact of transformed cells as CD23 was found associated with exosomes from primary mouse B cells (Fig. 5*A*), nor is it specific to one species, as CD23 containing exosomes are secreted from both human and mouse B cells.

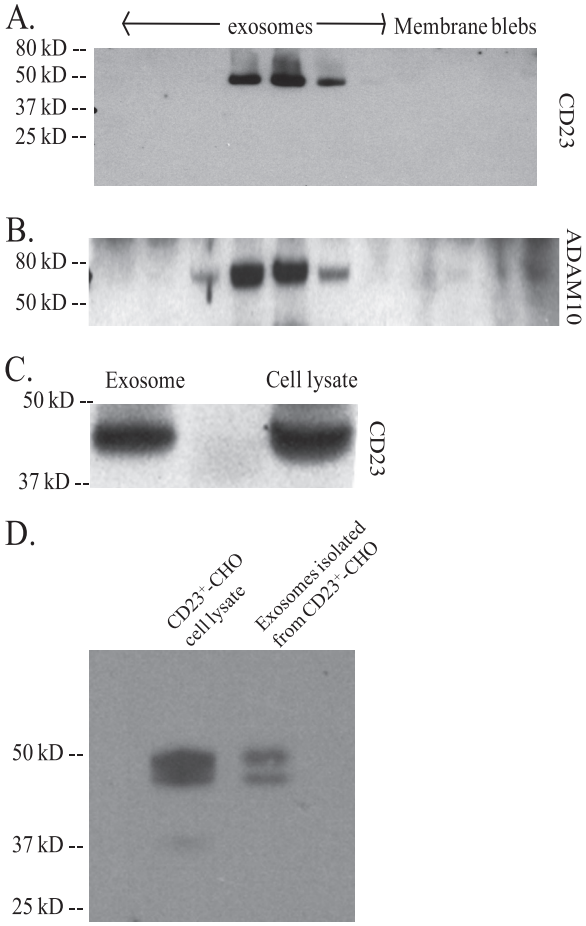

FIGURE 3. **Full-length CD23 was found in B-cell secreted exosomes.** *A*, exosomes were isolated by ultracentrifugation from overnight cultures of RPMI 8866 cells, a human B-cell line. Exosomes where overlaid onto a discontinuous sucrose gradient as explained under "Experimental Procedures." Following centrifugation, fractions were collected and analyzed for the presence of CD23. *B*, the blot was stripped and also analyzed for ADAM10 with rabbit anti-ADAM10. *C*, to confirm that CD23 in exosomes was full-length, CD23 from cell lysate of RPMI 8866 was compared with CD23 from exosomes. *D*, exosomes from mouse CD23$^+$-CHO cells where CD23 had been destabilized with 19G5 were isolated, lysed in HBS containing 0.5% Nonidet P-40, and protease inhibitors. CD23 was then precipitated with 2H10-Affi-Gel and visualized by Western blot. For comparison, total CD23 was isolated from the same cells by immunoprecipitation of CD23 from CD23$^+$-CHO Nonidet P-40 lysates. The blots are representative of at least two experiments of similar design.

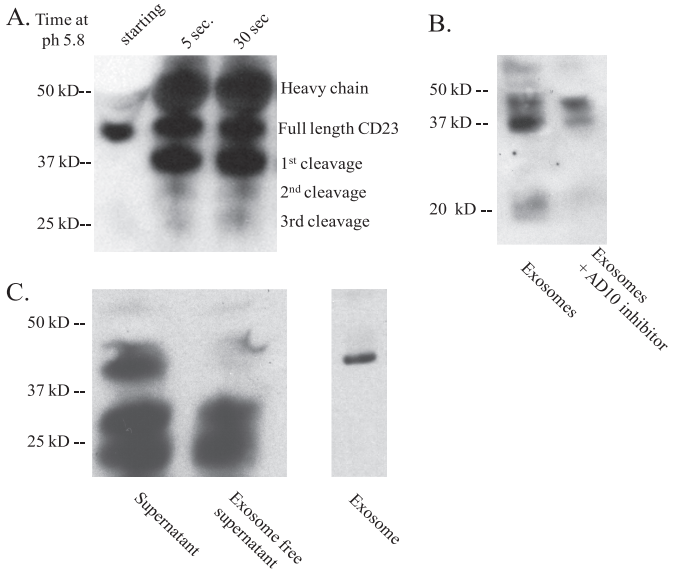

FIGURE 4. **CD23 was cleaved in exosomes in an ADAM10-dependent manner.** *A*, exosomes from RPMI 8866 supernatants were isolated and either lysed directly in SDS or resuspended in MES-buffered saline plus 1% serum and cultured at 37 °C for either 5 or 30 s. Cultures were then neutralized with Tris buffer (pH 8.0) and CD23 was immunoprecipitated with IDEC-152, and analyzed for CD23 by Western blot. *B*, exosomes from surface-biotinylated RPMI 8866 were isolated and resuspended in medium ± 10 μM ADAM10 inhibitor (INCB8765) and incubated at 37 °C for 17 h. Biotinylated proteins were then precipitated using avidin-agarose and analyzed for CD23 by Western blot. *C*, CD23 from RPMI 8866 cell-free supernatant or supernatant where exosomes had been removed were precipitated with IDEC-152 and compared with CD23 from exosomes via Western blot. The blots are representative of at least two independent experiments.

Demonstration of ADAM10-dependent Cleavage of Exosome CD23—As the size of CD23 found in exosomes corresponded to full-length CD23 (Fig. 3*C*), we examined CD23 cleavage by ADAM10 post-exosome incorporation. Exosomes from cultured RPMI 8866 cells were isolated from the supernatant and then resuspended for different periods of time in MES-buffered saline (50 mM MES, 100 mM NaCl) (pH 5.8) or RPMI (pH 7.4) containing heat-inactivated fetal calf serum. After neutralization, all samples were kept on ice and CD23 fragments were isolated and examined by Western blot (Fig. 4*A* and supplemental Fig. S2). The results were quite striking. When the exosomes were resuspended at pH 7.4 there was minimal cleavage, even after overnight culture at 37 °C. In contrast, the initial 37-kDa cleavage fragment is rapidly apparent if the exosomes are resuspended at pH 5.8, which mimics endosomal conditions. Not all of CD23 is cleaved, which explains why some CD23 is still released in the context of exosomes. Note also that the primary cleavage fragment observed is the first CD23 fragment reported by others (37). Some additional cleavage to 33 and 25 kDa is seen, but this is relatively minimal. Inclusion of the ADAM10 inhibitor in the exosome suspension blocked cleavage at pH 7.4 (Fig. 4*B*). The data thus demonstrates that ADAM10 is much more active at endosomal pH and suggests that some CD23 cleavage would take place before the exosomes are released from the cell. In addition, CD23 fragments were isolated from cell supernatant and exosome-free supernatants using anti-CD23, and examined by Western blot. In the exosome-free supernatants the primary fragments were the 33- and 25-kDa isoforms. These results demonstrate that ADAM-10-dependent cleaved fragments of CD23 seen in B cell cultures originates from the cleavage of exosome-associated CD23 after intact CD23 was sorted into exosomes. The data further suggest that the later CD23 fragmentation primarily occurred post-exosome release and are probably ADAM10 independent. This hypothesis of the later fragmentation being ADAM10 independent is in agreement with previous findings (38).

ADAM10 Was Essential for Sorting of CD23 into Exosomes—Previously B cells that lack ADAM10 were shown to have dramatically increased CD23 on the cell surface. In addition, the treatment of these cells with destabilizing antibodies did not cause an increase in cleavage (24) compared with WT. This indicates that ADAM10 might not only be important for cleavage of CD23, but also for sorting CD23 into exosomes. As seen earlier (Fig. 3*D*), full-length mouse CD23 is also included in exosomes. Thus, to test our hypothesis that ADAM10 is

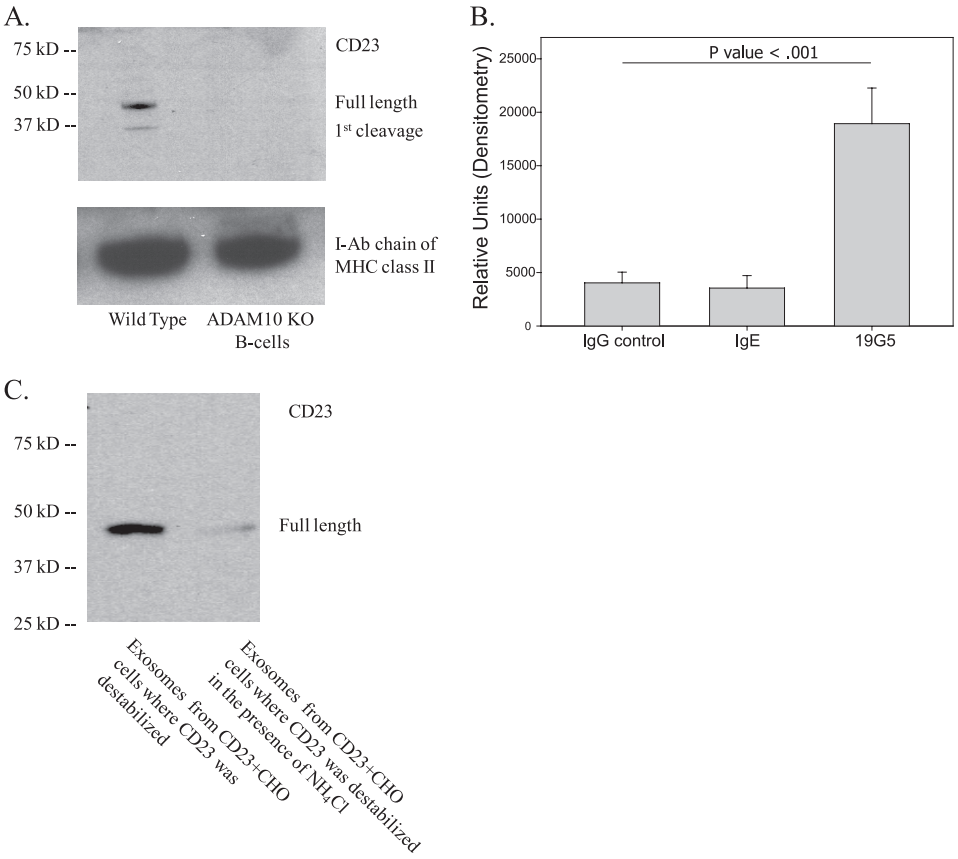

FIGURE 5. **ADAM10 binding of CD23 was essential for sorting into exosomes.** *A*, purified mouse B cells were isolated by fluorescence-activated cell sorting using anti-B220. They were then stimulated with LPS/IL-4 for 3 days. Exosomes were then isolated from the supernatant and analyzed for CD23 and MHC class II. *B*, equal amounts of mCD23^{+}-CHO cells were treated overnight with normal IgG or antibodies that either stabilize (IgE) or destabilize (19G5) CD23. Exosomes were then pelleted and analyzed for the amount of CD23 by Western blot. Shown is the average relative density of at least three independent experiments. *C*, mCD23^{+}-CHO cells were cultured ±10 mM NH_4Cl and destabilizing antibody (19G5) overnight; exosomes were then isolated and examined for the presence of CD23 by Western blot. Each blot is representative of at least three independent experiments.

required for inclusion in exosomes. B cells from CD19-cre$^{+/-}$-ADAM10$^{flox/flox}$ (ADAM10 KO) mice and Cre-negative littermates, used as WT control, were isolated and stimulated with LPS plus IL-4 for 3 days. Exosomes were then isolated and the presence of CD23 was determined by Western blot (Fig. 5*A*). In both situations exosomes were secreted, as seen by the presence of MHC class II, however, in the exosomes derived from the ADAM10 KO B cells, CD23 was not present. In addition, Fig. 5*B* demonstrates that enhanced CD23 incorporation into exosomes is seen under destabilizing (19G5) conditions, as compared with stabilized (IgE) or control (normal IgG). Finally, CD23 inclusion in exosomes could also be blocked by culturing mCD23^{+}-CHO cells in the presence of NH_4Cl (Fig. 5*c*). Overall, the data of Figs. 4 and 5 suggest that CD23 is first incorporated in the MVB into exosomes, and secreted as intact exosome-bound CD23. However, at endosomal pH, rapid ADAM10-dependent cleavage occurs. Once released, the initial cleavage is much more gradual, but is still ADAM10 dependent. These results thus showed that ADAM10 is essential for CD23 inclusion in exosomes, most likely through their direct interaction.

The Interaction of ADAM10 and CD23—We next sought to understand the mechanics of the ADAM10-CD23 interaction. All previously known ligands of CD23, including IgE, CD11, CD18, and CD21, bind CD23 in the lectin head. ADAM10 binds its substrates in a protease-independent manner, where binding takes place in the disintegrin or cysteine-rich regions (39). To investigate the binding sites of ADAM10 and CD23, an *in vitro* assay was used where recombinant trimerized mouse CD23 was trapped on nitrocellulose in a dot blot approach. Then after blocking with nonspecific proteins, ADAM10 was allowed to interact. The ADAM10 protein used for binding was from the cell lysate of 293F cells overexpressing ADAM10. After washing, bound ADAM10 was detected using anti-ADAM10. Using this approach we first demonstrated that the CD23-ADAM10 interaction could be determined in this manner (supplemental Fig. S3*A*), and confirms previous data (38), which found that CD23 and ADAM10 were co-precipitated in overexpressing cells. Next, to determine the regions of ADAM10 and CD23 important in binding, mutant recombinant fragments of CD23 (where either the lectin head or sections of the stalk region of CD23 were removed) were used in the dot blot approach and binding of ADAM10 was compared with full-length CD23 (Fig. 6*A*). The samples tested were *lz*-CD23$^{86-331}$, which represents full-length trimeric CD23 (30); *lz*-CD23$^{139-331}$, which was the mutant form that still contained the ADAM10 cleavage site and still interacted normally with IgE (30); CD23$^{48-171}$, which is the stalk region alone; and *lz*-CD23$^{171-331}$, which lack the ADAM10 cleavage site and no longer interacts with IgE (30). In contrast to IgE and other CD23 binding partners that require the lectin head for binding, the CD23 stalk alone bound ADAM10; showing that ADAM10 binds in the stalk region of CD23. Data from the other mutant fragments showed that this binding takes place between amino acids 139 and 171 of CD23. These data help explain earlier studies that indicated that the polyclonal rabbit anti-stalk blocked CD23 cleavage (11). Next using a similar approach, we used lysate from cells overexpressing dominant-negative ADAM10 (40) and showed that ADAM10 binds CD23 in a protease-independent manner (supplemental Fig. 3*B*). This demonstrated that ADAM10 binds CD23 similar to other substrates, namely in a protease-domain independent manner.

The dot blot approach was also used to determine whether destabilizing (19G5) or stabilizing (IgE) reagents would influence the interaction of ADAM10 and CD23. As is seen in Fig. 6*B*, 19G5 did not alter the level of interaction, further support-

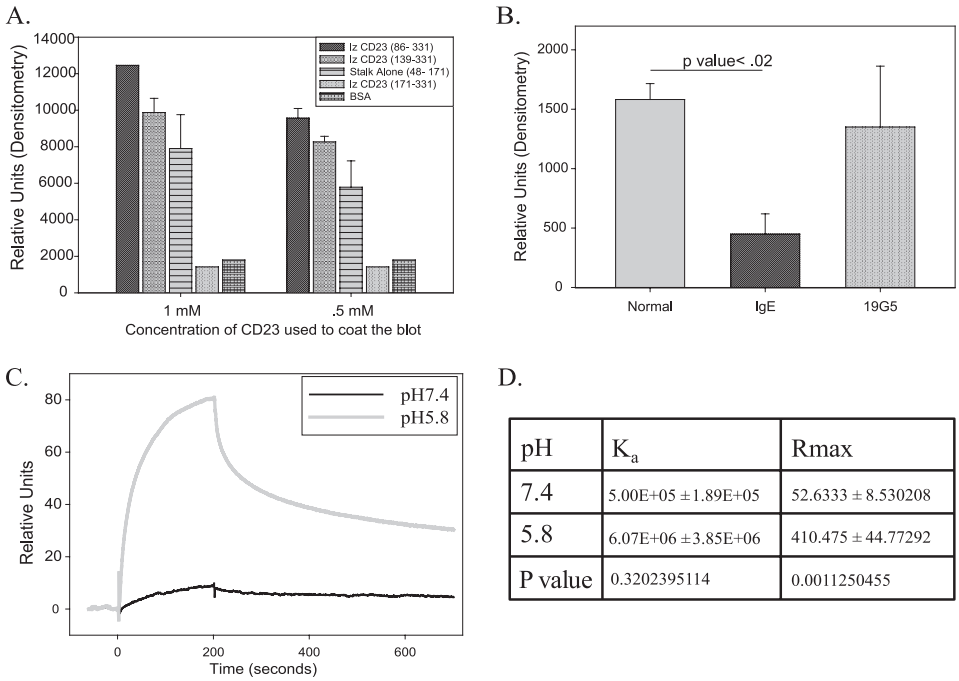

pH	K_a	Rmax
7.4	5.00E+05 ±1.89E+05	52.6333 ± 8.530208
5.8	6.07E+06 ±3.85E+06	410.475 ± 44.77292
P value	0.3202395114	0.0011250455

FIGURE 6. **ADAM10 binds the stalk region of CD23 in a protease-independent manner.** *A*, mutant forms of CD23 (*numbers* indicate amino acids included), using the procedure explained under supplemental Fig. S3, were added to the blot and binding was compared with the full-length CD23; shown are the relative densities of the respective spots and the average of two experiments is shown. *B*, CD23 on the blot was either stabilized or destabilized by incubation with IgE and 19G5, respectively, prior to the addition of ADAM10, and binding was compared with the untreated control; shown is the average relative density of three independent experiments. *C*, rADAM10 was immobilized on the chip and 5 μg/ml of recombinant CD23 was flowed over the top, diluted in either MES-buffered saline (pH 5.8) or HEPES-buffered saline (pH 7.4), and the sensogram, minus the control lane, for each was overlaid. *D*, binding of multiple concentrations (5–100 μg/ml) of recombinant CD23 was allowed to bind to immobilized rADAM10 and both the affinity and R_{max} were calculated under steady state calculations. Shown is the average of at least four independent experiments.

ing the concept that "destabilization" really reflects increased internalization. Intriguingly, IgE did partially block the interaction of ADAM10 and CD23. This suggests that IgE inhibits CD23 cleavage in a dual manner, both by keeping CD23 at the cell surface (Fig. 1*C*) and blocking ADAM10 interaction directly (Fig. 6*B*).

To extend and confirm the interaction data SPR analysis was used. Recombinant ADAM10 was immobilized on a CM5 chip and allowed to interact with recombinant CD23. The soluble CD23 that was used was *lz*-CD23$^{139-331}$, which was shown previously to be the minimal amount of stalk to refold in a trimeric form capable of interacting with IgE (30). In addition, this was the minimal amount of stalk needed for ADAM10 binding (Fig. 6*A*). As ADAM10-dependent CD23 cleavage was enhanced at endosomal pH, CD23 was dissolved in either pH 5.8 (the pH of MVB (33)) or the expected extracellular pH 7.4. Steady state affinity measurements were not significantly different when comparing the values obtained at either pH (Fig. 6*D*); however, the R_{max} value was about an order of magnitude higher at pH 5.8. An example sensogram comparison at the two pH values is shown in Fig. 6*C*. The large increase in R_{max} indicates that the site for ADAM10 binding is more accessible at the lower pH, whereas the similar affinities indicate that once accessible, the binding strength is not significantly different.

DISCUSSION

For the last 20 years CD23 has been the subject of intense study as a possible molecule in the regulation of IgE-mediated allergy, B cell lymphocytic leukemia (42), and arthritis (43). The focus on CD23 in the context of allergy, related to its ability to control IgE synthesis, has intensified recently with the success of anti-IgE in such patients (10). Anti-IgE does not alter IgE synthesis, thus injections have to be done frequently and makes it a very expensive treatment. Methods to control IgE synthesis could potentially enhance anti-IgE therapy when used in combination, or if the inhibition is sufficient, could be used alone. This lead to a clinical trial with anti-CD23, where inhibition of IgE levels was observed (44), however, this inhibition was insufficient in itself to moderate allergic symptoms. Combined trials have not been reported. One of the primary difficulties in utilizing CD23 as a mechanism to block IgE is its susceptibility to cleavage. With the discovery that ADAM10 is the protease primary responsible for CD23 cleavage (13) blocking this cleavage became a step closer to reality. In this study we have tried to define more about the mechanism of the ADAM10/CD23 interaction, with the ultimate hope of controlling IgE synthesis by blocking CD23 cleavage.

CD23 ability to be cleaved has often been termed its stability; when destabilized its cleavage is increased, whereas stabilizing does the converse. These results reported here help to clarify the mechanism of this observation. Basically with the addition of IgE (stabilizing) or 19G5 (de-stabilizing) to CD23$^+$ cells there is a change in internalization of CD23 (see Fig. 1*C*), this change is then reflective in the amount of CD23 associated with exosomes (Fig. 5*B*) and in soluble cleaved products. When CD23 is destabilized there is an increased amount of CD23 associated with exosomes. Conversely when CD23 is stabilized with monomeric IgE, CD23 associated with exosomes is decreased. These results also might help explain previous findings (15) that although destabilization was believed to cause CD23 to unravel at the cell surface, when destabilizing antibodies were added there was no change in *fluorescence resonance energy transfer* between different sections of the trimer. Thus, the data in this study suggest that anti-stalk reagents increase internalization into endosomes. At endosomal pH levels, the ADAM10 cleavage site is evidently much more exposed, as evidenced by the rapid cleavage when exosomal bound CD23 is resuspended at pH 5.8 (Fig. 4). When the pH is closer to neutrality (pH 7.4) cleavage is much slower. We note also that IgE partially inhibits ADAM10 and CD23 interaction (Fig. 6*b*), which suggests that the previous finding of internalized IgE/antigen complexed with CD23 being recycled to the cell surface (31) is partially

because it would decrease the binding of ADAM10 and thus be less efficiently incorporated into exosomes. Finally, CD23 inclusion in exosomes could also be blocked by growing $CD23^+$-CHO cells in the presence of NH_4Cl (Fig. 5*C*) helping to explain our results shown in Fig. 2*A*, where reduced cleavage is seen in the presence of this reagent. The SPR results were also quite informative. Although the steady state affinity was not significantly different at pH 5.8 *versus* 7.4, the R_{max} increased about an order of magnitude (Fig. 6*D*). This indicates that accessibility of the ADAM10 binding site of CD23 was greatly increased by the lower pH, perhaps due to unraveling of the trimer at the lower pH. Most anti-lectin mAbs result in CD23 stabilization, analogous to IgE, and decrease internalization and thereby, also inhibit CD23 cleavage. The mechanism responsible for internalization changes is unknown, but changing the conformation of the cytoplasmic domain is an intriguing possibility, as this domain was recently shown to control internalization (32). Internalized CD23 then enters clathrin-coated pits and the endosomal pathway (see Refs. 31 and 32 and Table 1). Here ADAM10 has a higher ability to bind CD23 as is evident by the increase in R_{max} (see Fig. 6, *C* and *D*). Once ADAM10 and CD23 interact sorting into exosomes occurs and the exosome is either secreted with intact CD23, or the CD23 is rapidly cleaved. In addition, with the use of an ADAM10 specific inhibitor, we showed that the first cleavages of CD23 were ADAM10 dependent (see Fig. 4*B*), whereas subsequent cleavage was by other proteases, which agrees with earlier published findings (38). These findings also beg the question if other ADAM10 substrates (*e.g.* notch, EGF, and LAG-3) might also bind ADAM10 with a higher R_{max} at a lower pH.

B cell-derived exosomes are not simply a budding of the MVB or simply fragments of the plasma membrane as their protein constituency is different from the plasma membrane. For example, classical Fc receptors and transferrin receptors are not found in exosomes (35). Thus, for proteins to be secreted in exosomes they require a sort signal. Little is known about the signals required for sorting into exosomes. What is known is that the COP9 signalosome (CSN)-associated protein CSN5 regulates the quantity of some of the proteins in exosomes including ubiquitinated heat shock protein 70 (45). Ubiquitination, however, is not required for MHC II sorting into exosomes (46). For the EGF receptor, a single amino acid was shown to be important for its inclusion in exosomes (35), but little else is understood. We show that a protease, ADAM10, was essential for CD23 to be included in exosomes (Fig. 5*A*). Of note, although we only saw a 80% drop in sCD23 when cells were cultured in medium containing NH_4Cl, this is the same percentage drop that was seen in the ADAM10 KO (24), and primary mouse B cells cultured in the presence of inhibitors of ADAM10 (13). This correlation indicates that ADAM10 cleavage of CD23 first involves sorting of CD23 into exosomes. Also of note, whereas ADAM10 was shown to be the primary CD23 sheddase in mice (13), when human B cells were cultured with ADAM10 inhibitors only a 50% decrease (13) in sCD23 was seen. A similar decrease was also seen when human B cells were cultured with NH_4Cl in this study (data not shown), showing that although in both systems ADAM10 cleavage in the endosomal pathway was the dominant way of removal of CD23 from the cell, there are possible other proteases besides ADAM10 that have this role. These could include MMP9 (47) and ADAM8 (48) as both have been shown to be able to cleave CD23. Finally, when calcium is influxed into the cell it causes the MVB to fuse with the plasma membrane and the exosomes to be released (1). It was shown previously (13) that the calcium ionophore, ionomycin, increases the levels of CD23 fragments in cell supernatant. Our findings may explain this observation, as ionomycin would increase the fusing of MVB and thus, the release of CD23 containing exosomes.

Once sorted into exosomes CD23 was either rapidly cleaved by ADAM10 or secreted from the cell where cleavage by mature ADAM10 still occurred, albeit more slowly. Although the exact role of CD23 in exosomes is not known, the exosomal bound intact CD23 would retain its high affinity/avidity for IgE and thus, be able to bind both free IgE and IgE immune complexes. Thus, this pathway could represent more than just a pathway to remove CD23 from the cell, as CD23 bound with IgE complexes represent a good target for dendritic cells and could help explain the increased antigen presentation capacity seen with IgE-antigen complexes (reviewed in Ref. 49). We are currently testing this hypothesis, by seeing if dendritic cells when cultured in the presence of exosomes that have bound IgE-antigen complexes can stimulate dendritic cell antigen presentation with subsequent T cell activation. In the case of parasite infection, such an increase in Ag presentation would be advantageous, especially as exosome secretion increases with B cell activation (4). However, in the context of Type I allergic disease, delivery of antigens to antigen presenting cells by exosomal CD23 would be expected to cause increased reactions to allergens. Thus, blocking CD23 inclusion in exosomes through blocking of the internalization of CD23, analogous to IgE (Figs. 1*C* and 2*B*), is a possible allergy therapeutic strategy.

Anti-lectin mAbs have been used to try blocking cleavage and thus, IgE synthesis with some varied degrees of success. In rats, anti-CD23 was able to cause a 90% drop in antigen-specific IgE, while having no affects on other isotypes (50). However, in a clinical trial with an antibody against the lectin head of human CD23, Lumiliximab, there was only a 40% drop in IgE (44), which is not sufficient for clinical efficacy. This is possibly because anti-lectins do not block ADAM10-independent cleavage of CD23 and/or are not sufficiently effective in blocking internalization. In contrast to antibodies against the CD23 lectin domain, anti-stalk (destabilizing) caused enhanced CD23 cleavage in both the mouse (8) and human (12) and injection of anti-stalk into mice caused significant increases in serum IgE levels (8). All of this data are consistent with a regulatory role for the membrane-bound CD23. Decreased internalization in the presence of anti-lectin or IgE relates to the higher cell surface expression (Fig. 1*C*). This decrease in internalization would explain the decrease in IgE seen with anti-CD23 treatment, as CD23 must be kept at the surface as a trimer to regulate IgE (11). Alternatively, increased internalization, as seen with anti-stalk reagents, results in ADAM10-mediated sorting into exosomes (Fig. 5*A*). CD23 cleavage by ADAM10 in the exosomes resulted in the 37-kDa supernatant fragments that

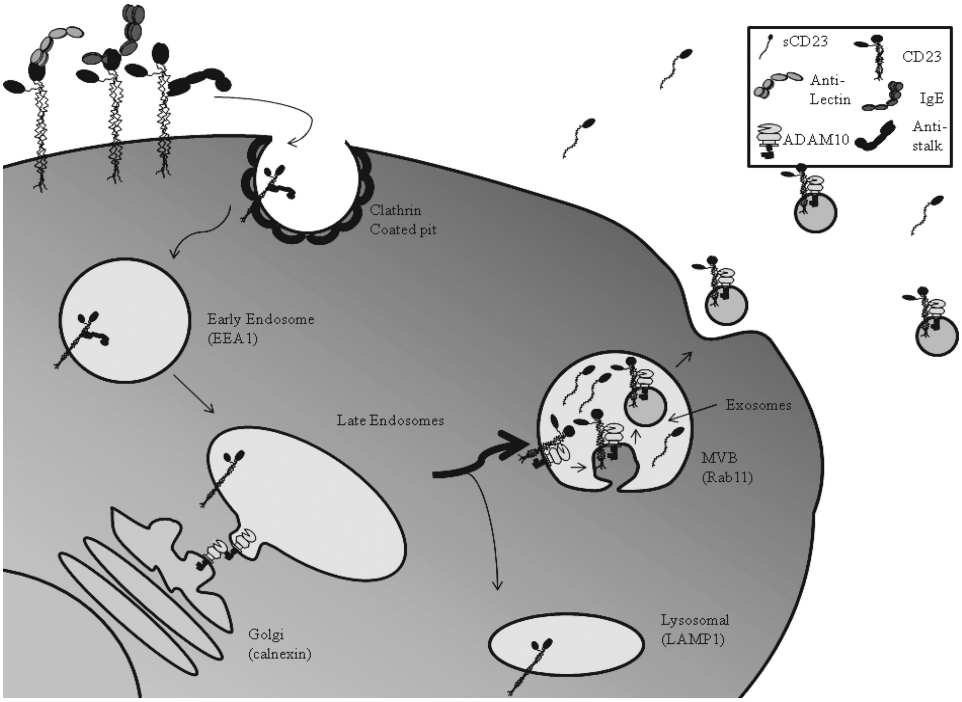

FIGURE 7. **Model for CD23 entering the endosomal pathway and in contact with ADAM10.** With the decrease in pH ADAM10 has increased accessibility to bind CD23 resulting in cleavage and/or sorting into exosomes. Exosome and endosomal contents are released from the cell; this process is enhanced by cell activation and calcium influx.

are seen (see Fig. 4*A*). Such increased cleavage correlates with higher IgE production in both mouse (8) and human systems (12).

As part of this study we also explored alternative ways of inhibiting CD23 inclusion in exosomes. One alternative is to keep CD23 on the surface (IgE or anti-lectin binding), thus, preventing it from coming in contact with ADAM10. High CD23 cell surface expression correlates with lower IgE synthesis. An additional alternative would be to block ADAM10 binding. This approach would be anticipated to increase cell surface CD23 levels; indeed B cells that lack ADAM10 were shown to have quite high cell surface CD23 (24). These studies indicate a mechanism for this cell surface increase, namely, ADAM10$^{-/-}$ B cells do not incorporate or secrete CD23 in exosomes and thus, blocking ADAM10 binding or cleavage is a second possible therapeutic target to regulate IgE synthesis. Although we only investigated the requirement of ADAM10 for CD23 inclusion in exosomes, we would hypothesize that ADAM10 would also be required for the other ADAM10 substrates known to be included in exosomes, L1 and CD44 (14); thus, as these molecules are important in human carcinoma motility and growth, blocking ADAM10 is a possible therapeutic approach in certain cancers. In addition, as exosomes have been shown to contain enzymatically active ADAM17 (14) it is possible that one role of the ADAMs is to sort proteins into exosomes. To block ADAM10 binding it has previously been found that an acidic pocket of the cysteine-rich region is important for binding, with three residues being specifically important (Glu-573, Glu-578, and Glu-579) (41). As we found that ADAM10 bound CD23 in a protease-independent manner, it is possible that this same region is also important for binding CD23 (see supplemental Fig. 3*B*) as this region could be targeted specifically. In addition, *N*-glycosylation of amino acid 280 of ADAM10 has been shown to be essential for ADAM10 shedding and sorting into exosomes. The mutation of this amino acid caused ADAM10 to be retained in the Golgi (23), offering another target region in blocking the ability of ADAM10 to cleave CD23.

In summary (Fig. 7), we show that CD23 internalization is affected by its stability. Once internalized CD23 was trafficked to the MVB where ADAM10, because of the change in pH, has increased access to bind and sort CD23 into exosomes; it was either rapidly cleaved or secreted as intact CD23 bound to exosomes. Calcium influx enhances this exosome secretion, helping to explain the increase in sCD23 production post cell activation. Once secreted, cleavage is more gradual and the subsequent cleavages are ADAM independent. Blocking this cleavage represents a novel way of increasing surface CD23 and decreasing IgE synthesis.

Acknowledgments—We thank Dr. Kirk Hauser for help with fluorescence imaging. We also thank Dr. John Tew for critical reviews of the manuscript.

REFERENCES

1. Théry, C., Zitvogel, L., and Amigorena, S. (2002) *Nat. Rev. Immunol.* **2,** 569–579
2. Viaud, S., Théry, C., Ploix, S., Tursz, T., Lapierre, V., Lantz, O., Zitvogel, L., and Chaput, N. (2010) *Cancer Res.* **70,** 1281–1285
3. Clayton, A., Turkes, A., Dewitt, S., Steadman, R., Mason, M. D., and Hallett, M. B. (2004) *FASEB J.* **18,** 977–979
4. McLellan, A. D. (2009) *Crit. Rev. Immunol.* **29,** 203–217
5. Saunderson, S. C., Schuberth, P. C., Dunn, A. C., Miller, L., Hock, B. D., MacKay, P. A., Koch, N., Jack, R. W., and McLellan, A. D. (2008) *J. Immunol.* **180,** 8146–8152
6. Muntasell, A., Berger, A. C., and Roche, P. A. (2007) *EMBO J.* **26,** 4263–4272
7. Conrad, D. H., Ford, J. W., Sturgill, J. L., and Gibb, D. R. (2007) *Curr. Allergy Asthma Rep.* **7,** 331–337
8. Ford, J. W., Kilmon, M. A., Haas, K. M., Shelburne, A. E., Chan-Li, Y., and Conrad, D. H. (2006) *Cell. Immunol.* **243,** 107–117
9. Bonnefoy, J. Y., Gauchat, J. F., Life, P., Graber, P., Aubry, J. P., and Lecoanet-Henchoz, S. (1995) *Int. Arch. Allergy Immunol.* **107,** 40–42
10. Gould, H. J., and Sutton, B. J. (2008) *Nat. Rev. Immunol.* **8,** 205–217
11. Kilmon, M. A., Ghirlando, R., Strub, M. P., Beavil, R. L., Gould, H. J., and Conrad, D. H. (2001) *J. Immunol.* **167,** 3139–3145
12. Munoz, O., Brignone, C., Grenier-Brossette, N., Bonnefoy, J. Y., and Cousin, J. L. (1998) *J. Biol. Chem.* **273,** 31795–31800
13. Weskamp, G., Ford, J. W., Sturgill, J., Martin, S., Docherty, A. J., Swendeman, S., Broadway, N., Hartmann, D., Saftig, P., Umland, S., Sehara-Fujisawa, A., Black, R. A., Ludwig, A., Becherer, J. D., Conrad, D. H., and

Blobel, C. P. (2006) *Nat. Immunol.* **7,** 1293–1298
14. Stoeck, A., Keller, S., Riedle, S., Sanderson, M. P., Runz, S., Le Naour, F., Gutwein, P., Ludwig, A., Rubinstein, E., and Altevogt, P. (2006) *Biochem. J.* **393,** 609–618
15. Kilmon, M. A., Shelburne, A. E., Chan-Li, Y., Holmes, K. L., and Conrad, D. H. (2004) *J. Immunol.* **172,** 1065–1073
16. Schwartz, W., Jiao, J., Ford, J., Conrad, D., Hamel, J. F., Santabien, P., Bradbury, L., and Robin, T. (2004) *BioProcessing J.* **3,** 53–62
17. Liu, F. T., Bohn, J. W., Ferry, E. L., Yamamoto, H., Molinaro, C. A., Sherman, L. A., Klinman, N. R., and Katz, D. H. (1980) *J. Immunol.* **124,** 2728–2737
18. Kelly, A. E., Chen, B. H., Woodward, E. C., and Conrad, D. H. (1998) *J. Immunol.* **161,** 6696–6704
19. Zhou, B. B., Peyton, M., He, B., Liu, C., Girard, L., Caudler, E., Lo, Y., Baribaud, F., Mikami, I., Reguart, N., Yang, G., Li, Y., Yao, W., Vaddi, K., Gazdar, A. F., Friedman, S. M., Jablons, D. M., Newton, R. C., Fridman, J. S., Minna, J. D., and Scherle, P. A. (2006) *Cancer Cell* **10,** 39–50
20. Horiuchi, K., Le Gall, S., Schulte, M., Yamaguchi, T., Reiss, K., Murphy, G., Toyama, Y., Hartmann, D., Saftig, P., and Blobel, C. P. (2007) *Mol. Biol. Cell* **18,** 176–188
21. Pan, D., and Rubin, G. M. (1997) *Cell* **90,** 271–280
22. Poole, J. A., Meng, J., Reff, M., Spellman, M. C., and Rosenwasser, L. J. (2005) *J. Allergy Clin. Immunol.* **116,** 780–788
23. Escrevente, C., Morais, V. A., Keller, S., Soares, C. M., Altevogt, P., and Costa, J. (2008) *Biochim. Biophys. Acta* **1780,** 905–913
24. Gibb, D. R., El Shikh, M., Kang, D. J., Rowe, W. J., El Sayed, R., Cichy, J., Yagita, H., Tew, J. G., Dempsey, P. J., Crawford, H. C., and Conrad, D. H. (2010) *J. Exp. Med.* **207,** 623–635
25. Dierks, S. E., Bartlett, W. C., Edmeades, R. L., Gould, H. J., Rao, M., and Conrad, D. H. (1993) *J. Immunol.* **150,** 2372–2382
26. Patki, V., Virbasius, J., Lane, W. S., Toh, B. H., Shpetner, H. S., and Corvera, S. (1997) *Proc. Natl. Acad. Sci. U.S.A.* **94,** 7326–7330
27. Kannan, K., Stewart, R. M., Bounds, W., Carlsson, S. R., Fukuda, M., Betzing, K. W., and Holcombe, R. F. (1996) *Cell. Immunol.* **171,** 10–19
28. Savina, A., Vidal, M., and Colombo, M. I. (2002) *J. Cell Sci.* **115,** 2505–2515
29. Krijnse-Locker, J., Parton, R. G., Fuller, S. D., Griffiths, G., and Dotti, C. G. (1995) *Mol. Biol. Cell* **6,** 1315–1332
30. Chen, B. H., Ma, C., Caven, T. H., Chan-Li, Y., Beavil, A., Beavil, R., Gould, H., and Conrad, D. H. (2002) *Immunology* **107,** 373–381
31. Karagiannis, S. N., Warrack, J. K., Jennings, K. H., Murdock, P. R., Christie, G., Moulder, K., Sutton, B. J., and Gould, H. J. (2001) *Immunology* **103,** 319–331
32. Montagnac, G., Mollà-Herman, A., Bouchet, J., Yu, L. C., Conrad, D. H., Perdue, M. H., and Benmerah, A. (2005) *J. Immunol.* **174,** 5562–5572
33. Ohkuma, S., and Poole, B. (1978) *Proc. Natl. Acad. Sci. U.S.A.* **75,** 3327–3331
34. Gutwein, P., Mechtersheimer, S., Riedle, S., Stoeck, A., Gast, D., Joumaa, S., Zentgraf, H., Fogel, M., and Altevogt, D. P. (2003) *FASEB J.* **17,** 292–294
35. Keller, S., Sanderson, M. P., Stoeck, A., and Altevogt, P. (2006) *Immunol. Lett.* **107,** 102–108
36. Keegan, A. D., and Conrad, D. H. (1987) *J. Immunol.* **139,** 1199–1205
37. Letellier, M., Sarfati, M., and Delespesse, G. (1989) *Mol. Immunol.* **26,** 1105–1112
38. Lemieux, G. A., Blumenkron, F., Yeung, N., Zhou, P., Williams, J., Grammer, A. C., Petrovich, R., Lipsky, P. E., Moss, M. L., and Werb, Z. (2007) *J. Biol. Chem.* **282,** 14836–14844
39. Blobel, C. P. (2005) *Nat. Rev. Mol. Cell Biol.* **6,** 32–43
40. Le Gall, S. M., Bobé, P., Reiss, K., Horiuchi, K., Niu, X. D., Lundell, D., Gibb, D. R., Conrad, D., Saftig, P., and Blobel, C. P. (2009) *Mol. Biol. Cell* **20,** 1785–1794
41. Janes, P. W., Saha, N., Barton, W. A., Kolev, M. V., Wimmer-Kleikamp, S. H., Nievergall, E., Blobel, C. P., Himanen, J. P., Lackmann, M., and Nikolov, D. B. (2005) *Cell* **123,** 291–304
42. Sarfati, M., Bron, D., Lagneaux, L., Fonteyn, C., Frost, H., and Delespesse, G. (1988) *Blood* **71,** 94–98
43. Bansal, A. S., Ollier, W., Marsh, M. N., Pumphrey, R. S., and Wilson, P. B. (1993) *Immunology* **79,** 285–289
44. Rosenwasser, L. J., and Meng, J. (2005) *Clin. Rev. Allergy Immunol.* **29,** 61–72
45. Liu, Y., Shah, S. V., Xiang, X., Wang, J., Deng, Z. B., Liu, C., Zhang, L., Wu, J., Edmonds, T., Jambor, C., Kappes, J. C., and Zhang, H. G. (2009) *Am. J. Pathol.* **174,** 1415–1425
46. Gauvreau, M. E., Côté, M. H., Bourgeois-Daigneault, M. C., Rivard, L. D., Xiu, F., Brunet, A., Shaw, A., Steimle, V., and Thibodeau, J. (2009) *Traffic* **10,** 1518–1527
47. Jackson, L., Cady, C. T., and Cambier, J. C. (2009) *J. Immunol.* **183,** 2585–2592
48. Fourie, A. M., Coles, F., Moreno, V., and Karlsson, L. (2003) *J. Biol. Chem.* **278,** 30469–30477
49. Hjelm, F., Carlsson, F., Getahun, A., and Heyman, B. (2006) *Scand. J. Immunol.* **64,** 177–184
50. Flores-Romo, L., Shields, J., Humbert, Y., Graber, P., Aubry, J. P., Gauchat, J. F., Ayala, G., Allet, B., Chavez, M., and Bazin, H. (1993) *Science* **261,** 1038–1041